Tunable broadband metamaterial absorber consisting of ferrite slabs and a copper wire*

Yang Yong-Jun(杨拥军), Huang Yong-Jun(黄勇军)†, Wen Guang-Jun(文光俊), Zhong Jing-Ping(钟靖平), Sun Hai-Bin(孙海斌), and Oghenemuero Gordon

Key Laboratory of Broadband Optical Fiber Transmission & Communication Networks, School of Communication and Information Engineering, University of Electronic Science and Technology of China, Chengdu 611731, *China*

(Received 21 October 2011; revised manuscript received 16 November 2011)

A tunable broadband metamaterial absorber is demonstrated at microwave frequencies in this paper. The metamaterial absorber is composed of ferrite slabs with large resonance beamwidths and a copper wire. The theoretical analysis for the effective media parameters is presented to show the mechanism for achieving the perfect absorptivity characteristic. The numerical results of transmission, reflectance, and absorptivity indicate that the metamaterial absorber exhibits a near perfect impedance-match to free space and a high absorptivity of 98.2% for one layer and 99.97% for two layers at 9.9 GHz. The bandwidth with the absorptivity above 90% is about 2.3 GHz. Moreover, the absorption band can be shifted linearly in a wide frequency range by adjusting the magnetic bias. This metamaterial absorber opens a way to prepare perfectly matched layers for engineering applications.

Keywords: broadband metamaterial absorber, tunability, ferrite

PACS: 85.70.Ge, 41.20.Jb, 42.25.Bs **DOI:** 10.1088/1674-1056/21/3/038501

1. Introduction

The metamaterial absorber (MMA) consisting of artificial sub-wavelength composites[1,2] reported by Landy *et al.* in 2008[3] has attracted considerable attention in the past four years because of the controllable effective refractive index $n(\omega)$ and impedance $Z(\omega)$ and its potential applications, such as the perfectly matched layer (PML) and the bolometer.[3,4] Most up-to-date MMAs are composed of metallic electric resonators and cut wires or metallic plate layers at microwave,[5−16] terahertz,[17−20] infrared,[21] and optical frequencies.[22,23] Dual-band and the multi-band MMAs based on different electric resonators or the same resonators with different sizes have also been introduced.[24−33] Those MMAs are realized by using metallic electric resonators to absorb incident electric fields and cut wires or metallic plate layers to absorb incident magnetic fields. By adjusting the structural sizes of the metallic electric resonators and the cut wires or adjusting the distances between the electric resonators and the plate layers to achieve the conditions of effective permittivity $\varepsilon(\omega)$ equaling effective permeability $\mu(\omega)$, big dielectric loss $\tan\delta_\varepsilon$, and big magnetic loss $\tan\delta_\mu$, the MMAs can impedance-match the free space and absorb completely the incident electromagnetic (EM) waves. Such nearly perfect absorptivities are realized via numerical optimization methods using the commercial finite difference time domain (FDTD) solver Microwave Studio or the finite-element based electromagnetic solver (HFSS, Ansoft).

The MMAs mentioned above, however, are limited by their inherent narrow bandwidths and are not tunable at all, resulting from the inherent narrow resonance bandwidths of most metallic electric resonators.[3,5−15] Some researchers have presented broadband MMAs by using different resonators or the same resonators with different sizes to broaden the bandwidths,[16,31,34] however, they are still far from being dynamically tunable. Recently, on the other hand, a novel design for a tunable negative index metamaterial consisting of a ferrite and a continuous wire is presented.[35−39] The ferrite under an applied magnetic bias provides the broadband magnetic resonance, and the continuous wire embedded in the ferrite provides the electric resonance at the same frequency band. The negative index frequency band can be shifted by adjusting the magnetic bias. In our previous works, we have also demonstrated experimentally the novel properties of such ferrite based meta-

*Project supported by the National Natural Science Foundation of China (Grant No. 60571024).

†Corresponding author. E-mail: yongjunh@uestc.edu.cn

© 2012 Chinese Physical Society and IOP Publishing Ltd

materials and discussed the dual-band and the multi-band transmission characteristics.[40−42]

Such ferrite based metamaterials can also be used in the MMA to absorb the incident magnetic and electric fields by enlarging $\tan\delta_\mu$ and $\tan\delta_\varepsilon$, respectively. The absorption mechanism of the ferrite based MMA is distinctly different from that of the above mentioned electric resonator MMAs, because the incident magnetic field is absorbed by the ferrite slab, and the incident electric field is absorbed by the continuous copper wire embedded in the ferrite slab. Moreover, the absorption band of such an MMA can be expanded by choosing a special ferrite with a big resonance beamwidth and can also be tuned by adjusting the applied direct-current (dc) magnetic bias. In this paper, the new designed MMA consisting of a ferrite slab and a continuous copper wire is theoretically discussed, and the numerical results calculated by using Ansoft HFSS software are presented to demonstrate the theoretical analysis.

2. Model and theoretical analysis

The unit cell of the ferrite–wire MMA is shown in Fig. 1. A continuous copper wire with a thickness of 0.017 mm is printed in the center of the FR4 ($\epsilon_r = 4.4, \tan\delta = 0.02$) substrate, which has been widely used in conventional MMA design. Then the two sides of the FR4 substrate are deposited with two ferrite slabs (ferrite TT1-390 is used in this paper, with saturation magnetization $4\pi M_s = 2150$ G, $\epsilon_r = 12.7$, resonance beamwidth $\Delta H = 648$ Oe). An applied dc magnetic bias is applied on the ferrite slabs along the z axis to excite the magnetic anisotropy property. When an incident EM wave propagates along the y axis with the electric field along the z axis and the magnetic field along the x axis (shown in Fig. 1), the theoretical effective permeability of the ferrite slabs can be defined as $\mu_{\text{eff}} = (\mu^2 - \kappa^2)/\mu$, with $\mu = 1 + \omega_m\omega_0/(\omega_0^2 - \omega^2)$ and $\kappa = \omega_m\omega/(\omega_0^2 - \omega^2)$,[43] where $\omega_0 = \gamma H_0$ is the ferromagnetic resonance (FMR) frequency, γ denotes the gyromagnetic ratio, $\omega_m = 4\pi M_s\gamma$ stands for the characteristic frequency of the ferrite slabs, ω represents the angular frequency, and H_0 indicates the dc magnetic bias. For ferrite slabs with big resonance beamwidths, the damping describing the loss should be considered. So the FMR frequency is changed to $\omega_0 + j\alpha\omega$, where α denotes the damping of the ferromagnetic precession, $\alpha = \mu_0\gamma\Delta H/(2\omega)$.[44]

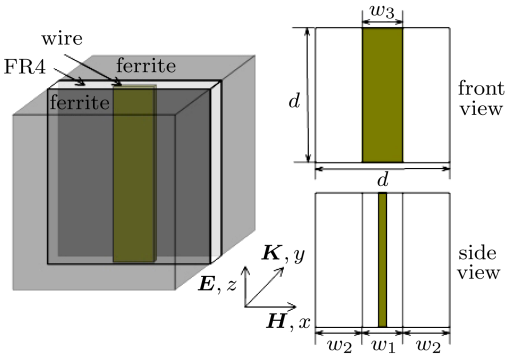


Fig. 1. (colour online) Schematic diagram of the ferrite–wire MMA unit cell. Front view, side view, and structure parameters are presented.

The effective permeability of the ferrite slab with resonance beamwidth ΔH and under a magnetic bias of 3.2 kOe is calculated as a function of frequency by using the above relations, and the results are presented in Fig. 2. It is shown that there is a magnetic resonance presented at 12 GHz and the real part of the effective permeability is clearly negative above

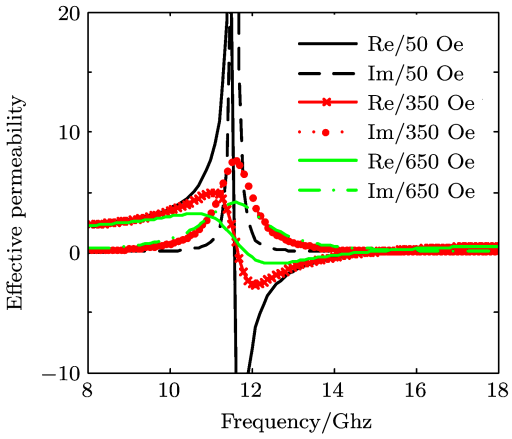


Fig. 2. (colour online) Calculated theoretical effective permeability of the ferrite slabs with different resonance beamwidth ΔH and under a magnetic bias of 3.2 kOe.

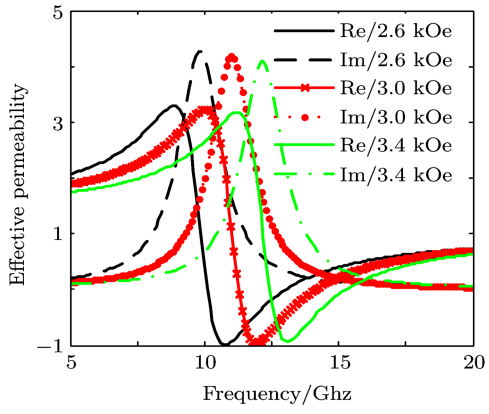


Fig. 3. (colour online) Calculated theoretical effective permeability of the ferrite slabs under different magnetic biases.

the magnetic resonance frequency. With the increase of ΔH, the effective magnetic loss tangent $\tan\delta_\mu = \mathrm{Im}(\mu)/|\mathrm{Re}(\mu)|$ increases rapidly in the region of negative permeability. For the ferrite slabs used in this paper, $\tan\delta_\mu$ has a value larger than 2.5 in the region of 12.3–14.3 GHz (not shown in Fig. 2). It means that the ferrite slabs can absorb most incident magnetic field. Moreover, the magnetic resonance of the ferrite slab can be shifted by adjusting the magnetic bias, as shown in Fig. 3. It can be observed that as the magnetic bias increases from 2.6 kOe to 3.4 kOe, the magnetic resonance shifts from 10 GHz to 12.5 GHz. The big $\tan\delta_\mu$ is retained well in the process of changing the magnetic bias. Therefore, the ferrite slabs provide the negative magnetic resonance to absorb the magnetic field of the incident EM wave and the tunable characteristics by adjusting the dc magnetic bias.

The effective permittivity of the wire embedded in the ferrite slabs can be expressed as[35]

$$\varepsilon_{\mathrm{eff}} = \epsilon_{\mathrm{f}} - \frac{\sigma_{\mathrm{eff}}/\omega}{\mathrm{i} + \left(\dfrac{\omega\mu_0 a^2\sigma_{\mathrm{eff}}}{2\pi}\right)\left[\ln\dfrac{r_2}{r_1} + \dfrac{\mu_{\mathrm{eff}}}{\mu_0}\left(\ln\dfrac{a}{r_2} - 1.06\right)\right]}, \tag{1}$$

where ϵ_{f} is the permittivity of the ferrite slab, σ_{eff} is the effective conductivity of the wire, r_1 and r_2 are the effective radii of the wire and the substrate layer, respectively, and a is the periodic lattice constant. So the effective permittivity of the wire can be calculated as a function of frequency, as shown in Fig. 4. It can be seen that the real part of the effective permittivity is negative in the wide region ranging from dc to 17 GHz. The effective dielectric loss tangent $\tan\delta_\varepsilon = \mathrm{Im}(\varepsilon)/|\mathrm{Re}(\varepsilon)|$ (also shown in Fig. 4) has a very large value ($\tan\delta_\varepsilon > 1$) in the range of 10–13 GHz. Therefore, the continuous wire under this condition can absorb most of the incident electric field. So the ferrite–wire MMA can absorb the incident EM waves, including the incident magnetic and electric fields, with a very high absorptivity.

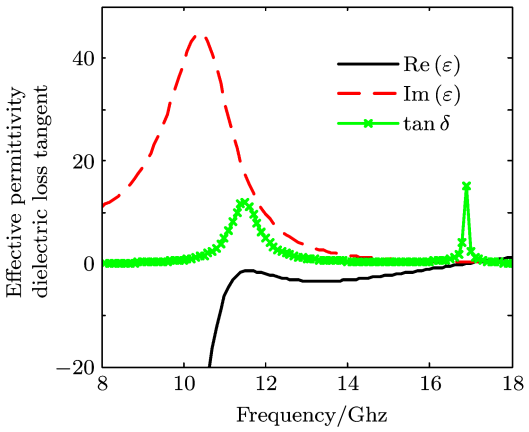


Fig. 4. (colour online) Calculated theoretical effective permittivity and effective dielectric loss tangent of the wire embedded in the ferrite slabs. Structural values are chosen as $r_1 = 0.6$ mm, $r_2 = 1$ mm, $a = 2.5$ mm.

The above analysis provides guidance for achieving the high absorptivity of the ferrite–wire MMA. Next, based on the above theoretical analysis, we further discuss the absorption characteristics by optimizing the parameters through a numerical method to achieve the perfect impedance-match and the highest absorptivity.

3. Numerical demonstrations

In the simulations, the commercial finite-element based electromagnetic solver (HFSS 11, Ansoft) is used to optimize the structure so that the MMA exhibits perfect absorption characteristics. The MMA unit cell is placed within a waveguide structure and excited by an EM wave with propagation vector $\boldsymbol{k}$ along the y axis, electric field vector $\boldsymbol{E}$ along the z axis, and magnetic field vector $\boldsymbol{H}$ along the x axis, as shown in Fig. 1. Accordingly, the walls perpendicular to the z axis are modeled to be perfect $\boldsymbol{E}$ boundaries, the walls perpendicular to the x axis are modeled to be perfect $\boldsymbol{H}$ boundaries, and the walls perpendicular to the y axis are modeled to be the input/output ports. A magnetic bias of 3.2 kOe is applied on the ferrite along the z axis.

The numerically optimized results of the MMA are shown in Fig. 5. The powers of transmission $T(\omega)$, reflectance $R(\omega)$, and absorptivity $A(\omega) = 1 - T(\omega) - R(\omega)$ are presented respectively. The final structure parameters are $d = 2$ mm, $w_1 = 0.959$ mm, $w_2 = 0.909$ mm, $w_3 = 0.585$ mm. It can be seen from Fig. 5 that both transmission $T(\omega)$ and reflectance $R(\omega)$ have very small values in the X band and so the absorptivity $A(\omega)$ has a very large value. The smallest value of reflectance $R(\omega)$ is about 0 at 9.9 GHz, so the MMA can be impedance-matched to the free

space perfectly. The peak value of absorptivity $A(\omega)$ is about 98.2% at 9.9 GHz, and the frequency band width of $A(\omega)$ over 90% is about 2.3 GHz. So this MMA can be called a broadband absorber. We note that the perfect absorbing frequency band in simulation is lower than the frequency band of theoretical large $\tan\delta_\mu$ and $\tan\delta_\varepsilon$. This is because the theoretical expressions given in Section 2 are for ideal conditions. The theoretical effective permeability is obtained for the ferrite slab only, and the theoretical effective permittivity is obtained for the model shown in Ref. [35]. So the theoretical expressions in this paper only provide the design guidance to achieve the absorbing characteristics, the optimized numerical results are more accurate for our MMA.

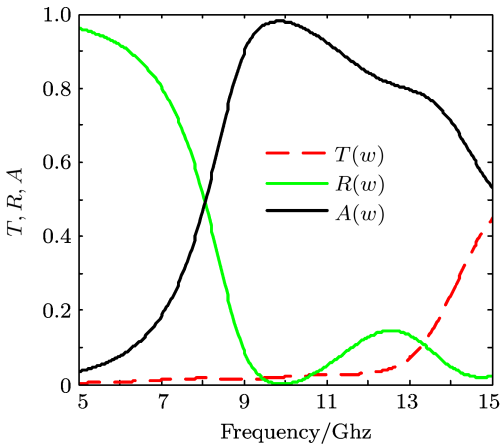


Fig. 5. (colour online) Simulated transmission, reflectance, and absorptivity characteristics of the ferrite–wire MMA under a magnetic bias of 3.2 kOe.

Moreover, the absorptivity can be further enhanced by adding layers of MMA together. Figure 6 shows the absorptivity characteristic as a function of the number of layers. As can be observed, $A(\omega)$ rises sharply with the additional layers and approaches asymptotically to 1. Two layers of the MMA can achieve an absorptivity of 99.92%. At this thickness, the entire structure is only $\lambda/5$ for the center operating frequency of 9.9 GHz.

In order to demonstrate the magneto-tunability of the absorbing frequency band, the MMA is simulated with different magnetic biases. Figure 7 shows the shift characteristic of the MMA in different magnetic biases. As shown in Fig. 7(a), the peak absorptivity and the bandwidth are not changed by the different magnetic biases. As shown in Fig. 7(b), the frequency of the peak absorptivity $A(\omega)$ shifts linearly from 6.75 GHz to 11.75 GHz as the magnetic bias changes from 2 kOe to 4 kOe with a linear tuning rate of 2.625 MHz/Oe. From Section 2, we know that the tunable characteristics of such a MMA mainly comes from the tunablility of the ferrite slabs under different magnetic biases. We expect that the ferrite–wire MMA can operate at higher frequencies, such as terahertz and far-infrared frequency bands with a similar broadband and tunable characteristics by using the terahertz ferrite films.[45]

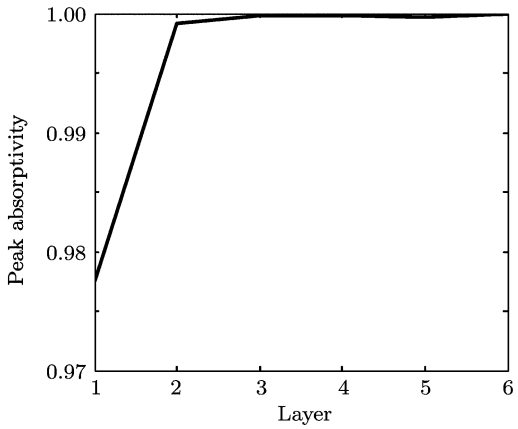


Fig. 6. Absorptivity characteristic of ferrite–wire MMA as a function of the number of layers.

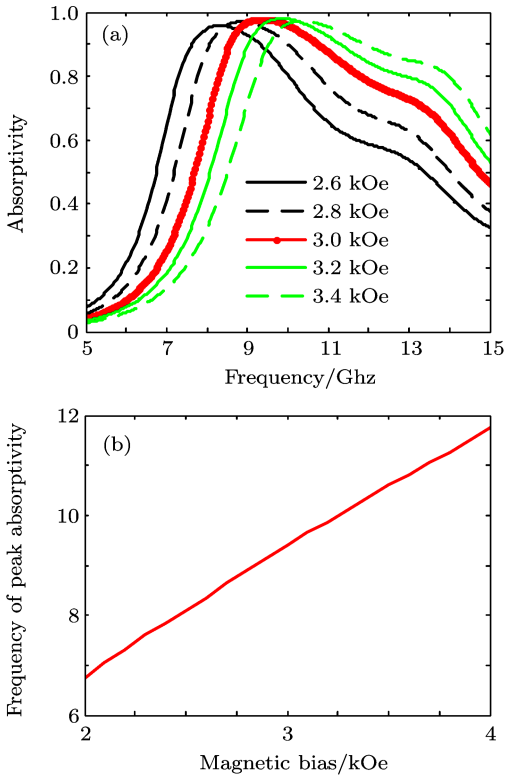


Fig. 7. (colour online) Peak shift properties of the absorptivity of the ferrite–wire MMA under different magnetic biases. (a) The absorption band characteristics under different magnetic biases, and (b) the frequency of the peak absorptivity as a function of the magnetic bias.

4. Conclusion

Based on the above theoretical analysis and the numerical simulation results, we conclude that the MMA presented in this paper exhibits very exciting characteristics, such as perfect impedance-match to the free space, high absorption, broadband, and tunable properties. The one layer thickness of such an MMA is just 2.777 mm (about $\lambda/10$ for the center operating frequency), and its peak absorptivity is 98.2%. By adding several absorber layers together, we can further enhance the absorptivity to near 100%. The bandwidth with the absorptivity over 90% for our MMA is about 2.3 GHz, and the band can be linearly shifted by adjusting the magnetic bias. Furthermore, the electrical size of each unit cell is just about 0.8, so it can be modeled as a homogeneous medium. The ferrites, the copper wire, the FR4 substrate, and the structural size are all available using the present techniques. All of the above advantages make the MMA applicable in various areas, e.g., it can be used to design a perfectly matched layer (PML) for engineering applications. A higher frequency MMA can also be achieved by using higher FMR ferrite films.

References

[1] Schurig D, Mock J J and Smith D R 2006 *Appl. Phys. Lett.* **88** 041109

[2] Padilla W J, Aronsson M T, Highstrete C, Lee M A, Taylor J and Averitt R D 2007 *Phys. Rev.* B **75** 041102

[3] Landy N I, Sajuyigbe S, Mock J J, Smith D R and Padilla W J 2008 *Phys. Rev. Lett.* **100** 207402

[4] Maier T and Brueckl H 2010 *Opt. Lett.* **35** 3766

[5] Zhu B, Wang Z B, Yu Z Z, Zhang Q, Zhao J M, Feng Y J and Jiang T 2009 *Chin. Phys. Lett.* **26** 114102

[6] Zhu B, Wang Z, Huang C, Feng Y, Zhao J and Jiang T 2010 *PIER* **101** 231

[7] Zhu W R, Zhao X P, Bao S and Zhang Y P 2010 *Chin. Phys. Lett.* **27** 014204

[8] Zhu W R and Zhao X P 2010 *Eur. Phys. J. Appl. Phys.* **50** 21101

[9] Hu C G, Li X, Feng Q, Chen X N and Luo X G 2010 *Opt. Express* **18** 6598

[10] Alici K B, Bilotti F, Vegni L and Ozbay E 2010 *J. Appl. Phys.* **108** 083113

[11] Cheng Y and Yang H 2010 *J. Appl. Phys.* **108** 034906

[12] Cheng Y, Yang H, Cheng Z and Wu N 2011 *Appl. Phys.* A **102** 99

[13] Gu C, Qu S B, Pei Z B, Zhou H, Xu Z, Bai P, Peng W D and Lin B Q 2010 *Chin. Phys. Lett.* **27** 117802

[14] Gu C, Qu S B, Pei Z B and Xu Z 2011 *Chin. Phys.* B **20** 037801

[15] Xu Y Q, Zhou P H, Zhang H B, Chen L and Deng L J 2011 *J. Appl. Phys.* **110** 044102

[16] Luo H, Wang T, Gong R Z, Nie Y and Wang X 2011 *Chin. Phys. Lett.* **28** 034204

[17] Tao H, Landy N I, Bingham C M, Zhang X, Averitt R D and Padilla W J 2008 *Opt. Express* **16** 7181

[18] Tao H, Bingham C M, Strikwerda A C, Pilon D, Shrekenhamer D, Landy N I, Fan K, Zhang X, Padilla W J and Averitt R D 2008 *Phys. Rev.* B **78** 241103

[19] Landy N I, Bingham C M, Tyler T, Jokerst N, Smith D R and Padilla W J 2009 *Phys. Rev.* B **79** 125104

[20] Grant J, Ma Y, Saha S, Lok L B, Khalid A and Cumming D R S 2011 *Opt. Lett.* **36** 1524

[21] Zhu W and Zhao X 2009 *J. Opt. Soc. Am.* B **26** 2382

[22] Zhu W, Zhao X, Gong B, Liu L and Su B 2011 *Appl. Phys.* A **102** 147

[23] Gong Y, Li Z, Fu J, Chen Y, Wang G, Lu H, Wang L and Liu X 2011 *Opt. Express* **19** 10193

[24] Wen Q Y, Zhang H W, Xie Y S, Yang Q H and Liu Y L 2009 *Appl. Phys. Lett.* **95** 241111

[25] Tao H, Bingham C M, Pilon D, Fan K, Strikwerda A C, Shrekenhamer D, Padilla W J, Zhang X and Averitt R D 2010 *J. Phys.* D: *Appl. Phys.* **43** 225102

[26] Li M H, Yang H L, Hou X W, Tian Y and Hou D Y 2010 *PIER* **108** 37

[27] He X J, Wang Y, Wang J M, Gui T L and Wu Q 2011 *PIER* **115** 381

[28] Ma Y, Chen Q, Grant J, Saha S C, Khalid A and Cumming D R S 2011 *Opt. Lett.* **36** 945

[29] Gu C, Qu S B, Pei Z B, Xu Z, Liu J and Gu W 2011 *Chin. Phys.* B **20** 017801

[30] Huang L and Chen H 2011 *PIER* **113** 103

[31] Luo H, Cheng Y Z and Gong R Z 2011 *Eur. Phys. J.* B **81** 387

[32] Li H, Yuan L H, Zhou B, Shen X P, Cheng Q and Cui T J 2011 *J. Appl. Phys.* **110** 014909

[33] Shen X P, Cui T J, Zhao J M, Ma H F, Jiang W X and Li H 2011 *Opt. Express* **19** 9401

[34] Bao S, Luo C R, Zhang Y P and Zhao X P 2010 *Acta Phys. Sin.* **59** 3187 (in Chinese)

[35] Dewar G 2005 *New J. Phys.* **7** 161

[36] Cai X M, Zhou X M and Hu G K 2006 *Chin. Phys. Lett.* **23** 348

[37] Rachford F J, Armstead D N, Harris V G and Vittoria C 2007 *Phys. Rev. Lett.* **99** 057202

[38] Zhao H J, Zhou J, Zhao Q, Li B, Kang L and Bai Y 2007 *Appl. Phys. Lett.* **91** 131107

[39] He Y X, He P, Yoon S D, Parimi P V, Rachford F J, Harris V G and Vittoria C 2007 *J. Magn. Magn. Mater.* **313** 187

[40] Huang Y J, Wen G J, Li T Q and Xie K 2010 *J. Electrom. Anal. Appl.* **2** 104

[41] Huang Y J, Wen G J, Li T Q and Xie K 2010 *Appl. Comput. Electrom. Soc. J.* **25** 696

[42] Huang Y J, Wen G J, Li T Q, Yang Y J and Xie K 2012 *Appl. Phys.* A **106** 79

[43] Lax B and Button K J 1962 *Microwave Ferrites and Ferrimagnetics* (New York: McGraw-Hill)

[44] Pozar D M 2005 *Microwave Engineering* (3rd Edn.) (New York: John Wiley & Sons, Inc) Chap. 9

[45] Yang Q H, Zhang H W, Liu Y L, Wen Q Y and Zha J 2008 *Chin. Phys. Lett.* **25** 3957